MICROCOPY RESOLUTION TEST CHART

NATIONAL BUREAU OF STANDARDS-1963-A

AFFDL-TR-76-151

BUCKLING OF CYLINDRICAL SANDWICH PANELS WITH LAMINATED FACES

UNIVERSITY OF DAYTON RESEARCH INSTITUTE

JANUARY 1977

TECHNICAL REPORT AFFDL-TR-76-151
FINAL REPORT FOR PERIOD NOVEMBER 1974 - OCTOBER 1975

DDC

RECEIVED

APR 19 1977

D

AIR FORCE FLIGHT DYNAMICS LABORATORY
AIR FORCE WRIGHT AERONAUTICAL LABORATORIES
AIR FORCE SYSTEMS COMMAND
WRIGHT-PATTERSON AIR FORCE BASE, OHIO 45433

This report has been reviewed by the Information Office (OI) and is releasable to the National Technical Information Service (NTIS). At NTIS, it will be available to the general public, including foreign nations.

This technical report has been reviewed and is approved for publication.

HAROLD C. CROOP
Project Engineer

LARRY G. KELLY, Acting Chief
Advanced Structures Development Branch
Structural Mechanics Division

FOR THE COMMANDER

HOWARD L. FARMER, Col, USAF
Chief, Structural Mechanics Division

REPORT DOCUMENTATION PAGE		READ INSTRUCTIONS BEFORE COMPLETING FORM
1. REPORT NUMBER AFFDL-TR-76-151	2 GOVT ACCESSION NO.	3. RECIPIENT'S CATALOG NUMBER
4. TITLE (and Subtitle) BUCKLING OF CYLINDRICAL SANDWICH PANELS WITH LAMINATED FACES.		5. TYPE OF REPORT & PERIOD COVERED Final Report 11/74 - 10/75
		6. PERFORMING ORG. REPORT NUMBER UDRI-TR-76-74
7. AUTHOR(s) R. A. Brockman		8. CONTRACT OR GRANT NUMBER(s) F33615-75-C-3009
9. PERFORMING ORGANIZATION NAME AND ADDRESS University of Dayton Research Institute 300 College Park Avenue Dayton, Ohio 45469		10. PROGRAM ELEMENT, PROJECT, TASK AREA & WORK UNIT NUMBERS Project No. 1368 Task No. 136802 Work Unit No. 13680217
11. CONTROLLING OFFICE NAME AND ADDRESS Air Force Flight Dynamics Laboratory, Advanced Structures Development Branch (FBS) Wright-Patterson AFB, Ohio 45433		12. REPORT DATE Jan 977
		13. NUMBER OF PAGES 53
14. MONITORING AGENCY NAME & ADDRESS(if different from Controlling Office)		15. SECURITY CLASS. (of this report) Unclassified
		15a. DECLASSIFICATION/DOWNGRADING SCHEDULE

16. DISTRIBUTION STATEMENT (of this Report)

Approved for public release; distribution unlimited.

17. DISTRIBUTION STATEMENT (of the abstract entered in Block 20, if different from Report)

18. SUPPLEMENTARY NOTES

19. KEY WORDS (Continue on reverse side if necessary and identify by block number)

structural analysis	cylindrical shells
structural sandwich composites	buckling
layered structure	elastic stability
sandwich panel	potential energy

20. ABSTRACT (Continue on reverse side if necessary and identify by block number)

General stability of a cylindrically curved sandwich panel with laminated composite face sheets is considered. The analysis accounts for axial compression, edgewise shear, or combined loadings. A mathematical model is formulated, based upon a linear potential energy expression and the Ritz method of discretization. Comparisons are made of the present method with a number of analytical and experimental buckling results. Limitations of the linear stability analysis are discussed in detail.

DD FORM 1473 1 JAN 73   EDITION OF 1 NOV 65 IS OBSOLETE

19. KEY WORDS (continued)
    Ritz Method
    combined loads
    curved panel
    simply supported
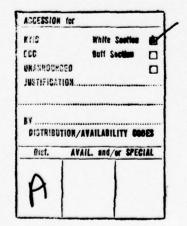
    edgewise compression
    edgewise shear

FOREWORD

TABLE OF CONTENTS

LIST OF FIGURES

LIST OF TABLES

LIST OF SYMBOLS

a	panel dimension parallel to generating axis
a_{ij}^{kl}	entries of elastic stiffness submatrices
b_s	circumferential dimension of layers of the panel
b_{ij}^{kl}	entries of geometric stiffness submatrices
c	subscript denoting core quantities
c_f	constant defined for each face sheet
d	total depth of sandwich panel
e_x, e_y	neutral surface parameters
f	subscript denoting face sheet quantities
h_{mn}, k_{mn}	assumed-mode coefficients
r	radial coordinate measured outward from the generating axis
s	subscript denoting a particular face or core layer of the sandwich panel
t_c	core thickness
t_f	face sheet thicknesses
u_s, v_s, w_s	midsurface displacement components for sandwich layers
x_s, y_s, z_s	local reference coordinates for layers
z	radial coordinate measured outward from the panel midsurface

A_1, A_2 — Lame' parameters of a surface

A_{ij} — elastic stiffness submatrices

A^{ij} — coefficient matrices from which the stiffness submatrices are constructed

$A_{ijf}, B_{ijf}, D_{ijf}$ — face sheet stiffness parameters for face f

B_{ij} — geometric stiffness submatrices

C_{ijf}^k — elastic constants for layer k of face f, with respect to principal material coordinate axes

E_{11f}^k, E_{22f}^k — elastic moduli for layer k of face f

E_f — elastic modulus of an isotropic face sheet

G_{xzc}, G_{yzc} — shear moduli of the sandwich core

G_{12f}^k — shear modulus for layer k of face f

H_{if} — functions defined for each face sheet

M_{xf}, M_{xyf}, M_{yf} — face sheet moment stress resultants

M_i, N_i — ranges of summation

N_{xf}, N_{xyf}, N_{yf} — face sheet membrane stress resultants

$N_{xf}^{(o)}, N_{xyf}^{(o)}$ — relative magnitudes of face sheet stresses immediately preceding buckling

$\overline{N}_x, \overline{N}_{xy}$ — magnitudes of total stress resultants immediately preceding buckling

Q_{ijf}^k — transformed elastic constants for layer k of face f

LIST OF SYMBOLS (Continued)

R_s	radius of curvature of surface s
R_o	radius of curvature of panel midsurface
U_s, V_s, W_s	displacement components at an arbitrary point in surface s
W_{mn}	assumed-mode coefficients
X_1, X_2	vectors of unknown coefficients
$\alpha_{fx}, \alpha_{fy}, \beta_f$	geometric parameters defined for each face sheet
γ_{ijs}	shear strain in surface s
γ_{ijs}^o	midsurface shear strain in surface s
δ	variational operator
δ_{ij}	Kronecker delta
$\epsilon_{xf}, \epsilon_{yf}$	extensional strains in face f
$\epsilon_{xf}^o, \epsilon_{yf}^o$	midsurface extensional strains in face f
θ	angular coordinate
$\varkappa_{xf}, \varkappa_{yf}, \varkappa_{xyf}$	curvature parameters for face f
λ	eigenvalue
ν_{ijf}^k	Poisson's ratios for layer k of face f
ν_f	Poisson's ratio of an isotropic face sheet
π_p	potential energy functional

LIST OF SYMBOLS (Concluded)

$\bar{\pi}_p$ discrete potential energy

σ_{xf}, σ_{yf} stresses in face f due to extension

τ_{xyf} shear stress in face f

ϕ, ψ core rotation parameters

Δ_{ij} defined operator

Θ panel included angle

Φ_{mn}, Ψ_{mn} assumed-mode coefficients

,   denotes partial differentiation with respect to the parameter following

SECTION 1

INTRODUCTION

The development of many types of low density, high strength
construction materials has provided numerous possibilities for efficient
structural design. Quite often, however, the full potential of these sophisti-
cated material concepts cannot be exploited, due to analytical shortcomings.
Economical and convenient analysis techniques are fast becoming the most
valuable tools of the structural designer. This observation is especially
true in view of current trends toward the development of automated design
procedures.

The practical applications of sandwich materials, in particular, have
outdistanced analytical capabilities to a considerable extent. A large body
of literature [1-4*] is concerned with the analysis of sandwich structures,
much of it devoted to the important question of elastic stability. However,
only the most basic geometries have been studied extensively. The stability
of flat sandwich panels [5-10] and of full cylinders [11-15], for example, have
received much attention. A few investigators have reported on the stability
analysis of open cylindrical shells [15-19], most often within the context of
a linear theory.

The present report describes the stability analysis of an open
cylindrical shell of a somewhat more general type than has been considered
previously. Numerical solutions are compared with numerous analytical
and experimental values. Some investigation is also made regarding the
limits of applicability of the linear buckling analysis for sandwich shells.

---

* Numerical superscripts indicate References listed at end of report.

1.1   PROBLEM DEFINITION

The present analysis addresses the problem of incipient general buckling of a cylindrical sandwich panel loaded by axial compression and edgewise shear forces. Each boundary of the shell is considered to be simply supported, and so constrained as to prevent shear within the core parallel to the panel edge. The component layers are confined to linear elastic response and small displacements, and are taken to be rigid in the direction normal to the surface of the panel.

The stiffnesses of the core in extension and bending are assumed to be sufficiently small that the core strain energy is due exclusively to transverse shear deformations. The transverse shear properties of the core may be different, as is the case in many practical situations.

The sandwich face sheets are considered as thin composite shells. That is, each face consists of a number of orthotropic layers, having different constitutive properties and arbitrary orientations with respect to the structural coordinate axes of the panel. Since the flexural rigidity of the faces about their own axes is included, the analysis may also be applied to the buckling problem of a laminated or isotropic shell. The face sheets are assumed to be thin in comparison to the radius of curvature of the panel, and to deform according to the Love-Kirchhoff assumptions.

1.2   METHOD OF SOLUTION

The mathematical model developed in this report is based upon the principle of minimum potential energy. The total potential energy of the panel, consisting of internal strain energy and the potentials of applied forces, is formulated in terms of the displacements within the sandwich core. The introduction of kinematically admissible assumed displacement modes into the potential energy yields a quadratic form in certain discrete displacement parameters. The discrete counterpart of the minimum potential energy principle, which requires that the gradient of this quadratic form

2

vanish, produces a set of algebraic equations of equilibrium, in the familiar form of a generalized eigenvalue problem. The critical load of least magnitude for the continuous structure is approximated by the smallest eigenvalue of the discrete system of equations. The corresponding eigen-vectors are approximations to the buckled displacement shapes which are the eigenfunctions of the continuous problem.

The displacement formulation used in the present analysis is a direct extension of the sandwich plate theory presented in Reference 20. This method has been employed in the buckling analysis of flat sandwich panels[21] with good results.

1.3 COMMENTS ON THE LINEAR THEORY OF STABILITY OF SHELLS

The classical stability theories of beams and plates are founded upon certain assumptions which are easily visualized as applicable to a wide class of practical problems. The consideration of shell stability by a linear theory is limited, however, by two particularly troublesome effects. The curvature of the shell surface couples transverse deflections with the in-surface displacements. Consequently, significant changes in the surface geometry may occur prior to the onset of instability, and indeed the buckling phenomenon itself is somewhat less clearly defined than for the case of plates or beams. Secondly, the curvilinear geometry tends to magnify the effects of the slightest deviations from a smooth initial configuration.[18] Typically, the influence of such imperfections is most pronounced for shells having severe curvature, and often the prediction of buckling by the linear theory is extremely inaccurate. When displacement coupling or irregularities are known to be significant, the use of a theory which considers these effects is appropriate.

The linear theory of shell stability, though restrictive by nature, does provide an economical method of analysis for problems in which the

effects of curvature are relatively small. For example, the shallow cylindrical shell geometry can often be analyzed by a linear theory with good results, since the deformations can closely resemble those of a flat plate.

The sensitivity of shell structures to initial geometry suggests that careful consideration be given to the analytical representation of the boundary conditions. The solution for simply-supported edges is often considered as a bounding case for panels which are supported in some manner along each edge; however, the presence of free edges or weak supports may have considerable effect upon the buckling behavior of curved panels.

The limitations mentioned in the linear theory of stability of shells should by no means be regarded as an indication that the theory is without value. Rather, the complex nature of the shell stability problem requires that the assumptions inherent in the linearization process be applied in a judicious manner, and only when appropriate, if meaningful results are to be obtained.

SECTION 2

DISPLACEMENT FORMULATION OF THE POTENTIAL ENERGY

In the formulation of the linear buckling problem, it is assumed that two pertinent equilibrium configurations can be identified. The initial equilibrium position is exactly that predicted by the classical linear theory of elasticity, while the second configuration corresponds to some "adjacent" state which is obtained from the first by virtue of some small perturbation. The phenomenon of buckling is viewed as a process of sudden transition between these two states of equilibrium. By adopting the first position of equilibrium as a reference state, and considering only those deformations which must occur during the excursion toward the adjacent state, the necessary conditions for the existence of the additional state of equilibrium are defined.

With this visualization of the problem, it is often appropriate to select as a reference state that configuration for which the prebuckling displacements have already occurred, and the critical stresses are present, in some specified proportions. In other words, the problem can be viewed as one of initial stress.[22] The critical load magnitudes are then taken to be that combination of the initial stresses for which some additional equilibrium position can be shown to exist. Accordingly, the displacement field which is considered represents that transition which occurs between the two equilibrium states; that is, the displacements due specifically to buckling. In the linear formulation of the problem, it is further assumed that the equilibrium state existing before the time of buckling is characterized by displacements which introduce only negligible changes in the geometry of the component.

2.1 GEOMETRY AND DISPLACEMENT

The cylindrical panel geometry is shown in Figure 1. The midsurfaces of the individual sandwich faces are selected as reference surfaces, having the local coordinates x_s, y_s, z_s. In terms of the global coordinates r, θ, x,

$$x_s = x$$
$$y_s = R_s \theta \qquad (2.1)$$
$$z_s = r - R_s; \qquad s = 1, 2, c.$$

A global coordinate $z = r - R_o$ is also employed, where R_o is the radius of curvature of the panel midsurface.

The face sheets are taken to be thin layers which obey the Love-Kirchhoff assumptions. Noting that the Lame' parameters of the shell are $A_1 = 1$, $A_2 = r$, the displacement at the generic point within face f is calculated from:

$$U_f = u_f - z_f w_{f,x}$$
$$V_f = v_f - z_f (w_{f,y} - \frac{v_f}{R_f}) \qquad (2.2)$$
$$W_f = w_f; \qquad f = 1, 2.$$

Since only general instability is to be considered, the variation in the transverse displacement through the thickness of the panel is neglected. That is,

$$w_1 = w_2 = w.$$

For the purpose of describing only those displacements which are due to the buckling deformation of the panel, it is assumed that displacements which occur prior to the onset of instability are small and introduce only negligible changes in the undeformed geometry. The uncoupling of these two sets of displacements is accomplished by postulating that there
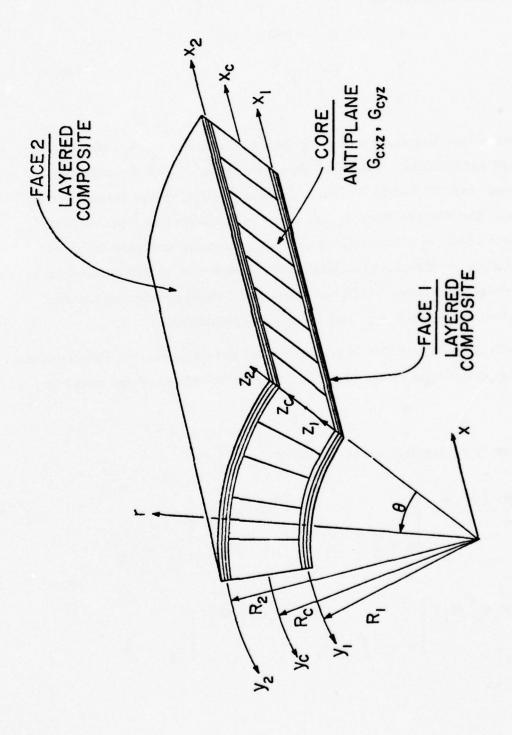
Figure 1

Panel Geometry and Coordinate System

exist certain "neutral" surfaces within the core layer, throughout which no insurface displacements are executed during the buckling deflection. In particular, it is assumed that

$$U_c = (z - e_x) \phi$$
$$V_c = (z - e_y) \psi \qquad (2.3)$$
$$W_c = w,$$

where ϕ and ψ are functions of the surface coordinates x_c, y_c, and e_x, e_y are constant parameters. Figure 2 shows the geometry of the assumed displacement state (Equation 2.3) at a section parallel to the straight edges of the panel. The displacement u_n indicated in the figure is a prebuckling displacement which is automatically excluded from the analysis by virtue of Equation 2.3. Notice that the functions ϕ and ψ can be interpreted as rotations of the core layer which are executed about points lying within the cylindrical surfaces $z = e_x$ and $z = e_y$, respectively.

The displacement fields in the faces and core are related by conditions of continuity at the bond lines. Letting the total thickness of the panel be

$$d = t_1 + t_2 + t_c,$$

the equations of continuity can be stated as

$$(U_c, V_c, W_c) \Big|_{z = \frac{d}{2} - t_2} = (U_2, V_2, W_2) \Big|_{z_2 = -\frac{t_2}{2}}$$

$$(2.4)$$

$$(U_c V_c, W_c) \Big|_{z = -\frac{d}{2} + t_1} = (U_1, V_1, W_1) \Big|_{z_1 = \frac{t_1}{2}}.$$

8
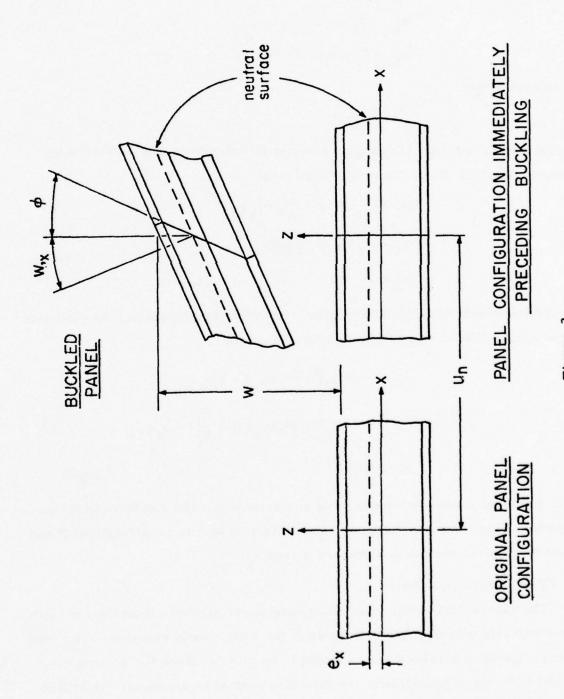
Figure 2

Geometry of Deformation

9

Defining

$$c_f = (-1)^{f+1}$$

$$\beta_f = \frac{d}{2} - t_f$$

$$\alpha_{fx} = \beta_f + c_f e_x \qquad (2.5)$$

$$\alpha_{fy} = \beta_f + c_f e_y \quad ; f = 1, 2,$$

and requiring that

$$R_f \gg \frac{t_f}{2} ,$$

the continuity conditions (Equations 2.4) can be solved to yield the following for the midsurface displacements of the faces:

$$u_f = -c_f (\alpha_{fx} \phi - \frac{1}{2} t_f w,_x)$$

$$v_f = -c_f (\alpha_{fy} \psi - \frac{1}{2} t_f w,_y) \qquad (2.6)$$

$$w_f = w_c = w \qquad\qquad ; f = 1, 2.$$

The displacements of an arbitrary point within the face sheets are then defined by the substitution of Equation 2.6 in Equation 2.2,

$$U_f = -c_f (\alpha_{fx} \phi - \frac{1}{2} t_f w,_x) - z_f w,_x$$

$$V_f = -c (\alpha_{fy} \psi - \frac{1}{2} t_f w,_y)(1 + \frac{z_f}{R_f}) - z_f w,_y \qquad (2.7)$$

$$W_f = w \qquad\qquad\qquad ; f = 1, 2.$$

Thus, the displacement components of any point within the sandwich panel can be expressed in terms of the transverse deflection w, the core rotations ϕ and ψ, and the neutral surface parameters e_x and e_y.

2.2 STRAIN AND STRESS

The extensional strains and in-surface shear strains within the sandwich core contribute only negligible amounts of the total elastic strain energy since the corresponding stresses are assumed to be small. Since the core is considered to be incompressible in the direction normal to the panel, the strain

10

energy due to deformations in this direction is also neglected. The remaining components of strain in the core are the transverse shear strains,

$$\gamma_{xzc} = U_{c,z} + W_{c,x}$$

$$\gamma_{yzc} = V_{c,z} + W_{c,y} - \frac{V_c}{r}.$$

$$(2.8)$$

Making use of Equation 2.3, the strain-displacement relations for the core can be written as

$$\gamma_{xzc} = \phi + w,_x$$

$$\gamma_{yzc} = \frac{1}{1 + z/R_c} (\psi + w,_y).$$

$$(2.9)$$

The corresponding shear stresses are calculated from

$$\tau_{xzc} = G_{xzc} \gamma_{xzc}$$

$$(2.10)$$

$$\tau_{yzc} = G_{yzc} \gamma_{yzc}$$

The strain-displacement relations for the face sheets are given by[23]

$$\epsilon_{xf} = \epsilon^o_{xf} + z_f \varkappa_{xf}$$

$$\epsilon_{yf} = \epsilon^o_{yf} + z_f \varkappa_{yf}$$

$$\gamma_{xyf} = \gamma^o_{xyf} + z_f \varkappa_{xyf}; \qquad f = 1, 2.$$

$$(2.11)$$

The midsurface strains and curvatures in Equation 2.11 are defined as

$$\epsilon^o_{xf} = u_{f,x}$$

$$\epsilon^o_{yf} = v_{f,y} + \frac{w}{R_f}$$

$$\gamma^o_{xyf} = v_{f,x} + u_{f,y}$$

$$(2.12)$$

11

$$\varkappa_{xf} = -w,_{xx}$$

$$\varkappa_{yf} = -w,_{yy} + \frac{v_{f,y}}{R_f} \tag{2.12}$$

$$\varkappa_{xyf} = -2(w,_{xy} - \frac{v_{f,x}}{R_f}) \; ; \; f = 1, \; 2,$$

where the midsurface face displacements u_f, v_f and w are defined in turn by Equation 2.6.

The generalized Hooke's law equations for a laminated face sheet are most conveniently represented in terms of the membrane stress resultants and moment stress resultants for the entire face. The development of these equations is given in Appendix A[*]. The resulting stress-strain relations are expressed in symbolic form as

$$\left\{ \frac{N_f}{M_f} \right\} = \left[\begin{array}{c|c} A_f & B_f \\ \hline B_f & D_f \end{array} \right] \left\{ \begin{array}{c} \epsilon^o_f \\ \varkappa_f \end{array} \right\} \; ; \; f = 1, \; 2. \tag{2.13}$$

2.3 POTENTIAL ENERGY

With the assumptions of Section 2.1, the reference configuration of the panel is identified as that state at which the critical loads have been applied, in certain specified proportions, but the displacements due to buckling have not yet occurred. Although the exact geometry of this reference configuration is not known unless a classical solution is performed, its deviation from the original (unstressed) state has been assumed to be sufficiently small as to be negligible. Thus the applied loads assume the character of initial, or residual, stresses, as noted previously.

The potential energy functional for an elastic body subjected to initial stresses $\lambda \sigma^{(o)}_x$ and $\lambda \tau^{(o)}_{xy}$ can be expressed as[22]

---

[*]Discussion and more detailed derivations of the constitutive equations for orthotropic laminates are widely available in the literature; see, for example, References 24-26.

$$\pi_p = \int \!\!\! \int \!\!\! \int_V \frac{1}{2} \left(\sigma_x \epsilon_x + \sigma_y \epsilon_y + \sigma_z \epsilon_z + \tau_{yz} \gamma_{yz} + \tau_{xz} \gamma_{xz} + \tau_{xy} \gamma_{xy} \right) \, dV$$

$$+ \lambda \int \!\!\! \int \!\!\! \int_V \frac{1}{2} \left[\sigma_x^{(o)} \left(u,_x^2 + v,_x^2 + w,_x^2 \right) \right. \tag{2.14}$$

$$\left. + 2 \tau_{xy}^{(o)} \left(u,_x u,_y + v,_x v,_y + w,_x w,_y \right) \right] \, dV$$

The functions $\sigma_x^{(o)}$ and $\tau_{xy}^{(o)}$ denote the relative magnitudes of the initially-applied stresses, while the parameter λ specifies the intensity of the loading. For the present problem, the region V includes both the face sheets and the core; making use of this fact, and the previous assumptions concerning stresses and strains, Equation 2.14 is restated in the form

$$\pi_p = \sum_{f=1}^{2} \int \!\!\! \int \!\!\! \int_{V_f} \frac{1}{2} \left(\sigma_{xf} \epsilon_{xf} + \tau_{xyf} \gamma_{xyf} + \sigma_{yf} \epsilon_{yf} \right) \, dV$$

$$+ \int \!\!\! \int \!\!\! \int_{V_c} \frac{1}{2} \left(\tau_{xzc} \gamma_{xzc} + \tau_{yzc} \gamma_{yzc} \right) \, dV_c \tag{2.15}$$

$$+ \lambda \sum_{f=1}^{2} \int \!\!\! \int \!\!\! \int_{V_f} \frac{1}{2} \left(\frac{N_{xf}^{(o)}}{t_f} w,_x^2 + 2 \frac{N_{xyf}^{(o)}}{t_f} w,_x w,_y \right) \, dV_f.$$

In Equation 2.15 it is assumed that the initial stresses are uniformly distributed through the face sheet thicknesses, and that the squares of derivatives of the insurface displacements are small in comparison with the squares of the transverse slopes. By introducing the stress-strain relations (Equations 2.10 and 2.13) into the potential energy, and performing the integrations through the panel thickness, the following is obtained:

13

$$\pi_p = \sum_{f=1}^{2} \int_o^b \int_o^a \frac{1}{2} \left\{ \begin{matrix} \epsilon_f^o \\ x_f \end{matrix} \right\}^T \left[\begin{array}{c|c} A_f & B_f \\ \hline B_f & D_f \end{array} \right] \left\{ \begin{matrix} \epsilon_f^o \\ x_f \end{matrix} \right\} dxdy$$

$$+ \int_o^b \int_o^a \frac{1}{2} \left(G_{xzc} t_c (\phi + w,_x)^2 + \frac{G_{yzc} t_c}{1 - \dfrac{\beta_1 \beta_2}{R_c^2}} (\psi + w,_y)^2 \right) dxdy$$

$$+ \lambda \sum_{f=1}^{2} \int_o^b \int_o^a \frac{1}{2} \left(N_{xf}^{(o)} w,_x^2 + 2N_{xyf}^{(o)} w,_x w,_y \right) dxdy \qquad (2.16)$$

It is important to notice that, in Equation 2.16, the variables and limits of integration refer to the local surface coordinates defined by Equation 2.1. That is,

$$x \equiv x_s$$
$$y \equiv y_s = R_s \theta,$$
$$b \equiv b_s = R_s \Theta; \ s = 1, \ 2, \ c,$$

if $\theta = 0$ and $\theta = \Theta$ and understood to be the bounding straight edges of the panel.

The displacement formulation of the potential energy is obtained from Equation 2.16 through the substitution of the strain-displacement expressions, Equations 2.6, 2.9, and 2.12. The resulting functional is

$$\pi_p = \sum_{f=1}^{2} \int_o^b \int_o^a \frac{1}{2} \left\{ \left[A_{11f}(\alpha_{fx}\phi,_x - \frac{1}{2}t_f w,_{xx})^2 + A_{22f}(\alpha_{fy}\psi,_y - \frac{1}{2}t_f w,_{yy})^2 \right. \right.$$

$$+ A_{66f}(\alpha_{fx}\phi,_y + \alpha_{fy}\psi,_x - t_f w,_{xy})^2$$

$$+ 2A_{12f}(\alpha_{fx}\phi,_x - \frac{1}{2}t_f w,_{xx})(\alpha_{fy}\psi,_y - \frac{1}{2}t_f w,_{yy})$$

$$+ 2A_{16f}(\alpha_{fx}\phi,_y + \alpha_{fy}\psi,_x - t_f w,_{xy})(\alpha_{fx}\phi,_x - \frac{1}{2}t_f w,_{xx})$$

14

$$+ 2A_{26f}(\alpha_{fx}\phi,_y + \alpha_{fy}\psi,_x - t_f w,_{xy})(\alpha_{fy}\psi,_y - \tfrac{1}{2}t_f w,_{yy})\Big]$$

$$+ 2c_f\Big[B_{11f}(\alpha_{fx}\phi,_x w,_{xx} - \tfrac{1}{2}t_f w,_{xx}^2)$$

$$+ B_{22f}(\alpha_{fy}\psi,_y w,_{yy} - \tfrac{1}{2}t_f w,_{xx}^2)$$

$$+ 2B_{66f}(\alpha_{fx}\phi,_y w,_{xy} + \alpha_{fy}\psi,_x w,_{xy} - t_f w,_{xy}^2)$$

$$+ B_{12f}(\alpha_{fy}\psi,_y w,_{xx} + \alpha_{fx}\phi,_{yy} - t_f w,_{xx}w,_{yy})$$

$$+ B_{16f}(\alpha_{fx}\phi,_y w,_{xx} + \alpha_{fy}\psi,_x w,_{xx} - t_f w,_{xy}w,_{xx})$$

$$+ B_{26f}(\alpha_{fx}\phi,_y w,_{yy} + \alpha_{fy}\psi,_x w,_{yy} - t_f w,_{xy}w,_{yy})$$

$$+ 2B_{16f}(\alpha_{fx}\phi,_x w,_{xy} - \tfrac{1}{2}t_f w,_{xx}w,_{xy})$$

$$+ 2B_{26f}(\alpha_{fy}\psi,_y w,_{xy} - \tfrac{1}{2}t_f w,_{yy}w,_{xy})\Big]$$

$$+ \frac{1}{R_f}\Big[\frac{A_{22f}}{R_f}w^2 - 2c_f\left(A_{22f} + \frac{B_{22f}}{R_f}\right)(\alpha_{fy}\psi,_y w - \tfrac{1}{2}t_f w w,_{yy})$$

$$+ \left(2B_{22f} + \frac{D_{22f}}{R_f}\right)(\alpha_{fy}\psi,_y - \tfrac{1}{2}t_f w,_{yy})^2 - 2B_{22f}w w,_{yy}$$

$$+ 2c_f D_{22f}(\alpha_{fy}\psi,_y w,_{yy} - \tfrac{1}{2}t_f w,_{yy}^2)$$

$$+ 4\left(B_{66f} + \frac{D_{66f}}{R_f}\right)(\alpha_{fy}\psi,_x - \tfrac{1}{2}t_f w,_{xy})^2$$

15

$$+ \ 4B_{66f}(\alpha_{fy}\psi,_x - \tfrac{1}{2}t_f w,_{xy})(\alpha_{fx}\phi,_y - \tfrac{1}{2}t_f w,_{xy})$$

$$+ \ 8c_f D_{66f}(\alpha_{fy}\psi,_x w,_{xy} - \tfrac{1}{2}t_f w,_{xy}^2)$$

$$- \ 2c_f A_{12f}(\alpha_{fx}\phi,_x w - \tfrac{1}{2}t_f w w,_{xx}) - 2B_{12f} w w,_{xx}$$

$$+ \ 2B_{12f}(\alpha_{fx}\phi,_x - \tfrac{1}{2}t_f w,_{xx})(\alpha_{fy}\psi,_y - \tfrac{1}{2}t_f w,_{yy})$$

$$+ \ 2c_f D_{12f}(\alpha_{fy}\psi,_y w,_{xx} - \tfrac{1}{2}t_f w,_{yy} w,_{xx})$$

$$+ \ 4B_{16f}(\alpha_{fx}\phi,_x - \tfrac{1}{2}t_f w,_{xx})(\alpha_{fy}\psi,_x - \tfrac{1}{2}t_f w,_{xy})$$

$$+ \ 4c_f D_{16f}(\alpha_{fy}\psi,_x w,_{xx} - \tfrac{1}{2}t_f w,_{xy} w,_{xx})$$

$$- \ 2c_f A_{26f}(\alpha_{fx}\phi,_y w - \tfrac{1}{2}t_f w w,_{xy}) - 4B_{26f} w w,_{xy}$$

$$- \ 2c_f \left(A_{26f} + 2\,\frac{B_{26f}}{R_f} \right)(\alpha_{fy}\psi,_x w - \tfrac{1}{2}t_f w w,_{xy})$$

$$+ \ 2B_{26f}(\alpha_{fx}\phi,_y - \tfrac{1}{2}t_f w,_{xy})(\alpha_{fy}\psi,_y - \tfrac{1}{2}t_f w,_{yy})$$

$$+ \ 4c_f D_{26f}(\alpha_{fy}\psi,_y - \tfrac{1}{2}t_f w,_{yy} w,_{xy})$$

$$+ \ 2 \left(3B_{26f} + 2\,\frac{D_{26f}}{R_f} \right)(\alpha_{fy}\psi,_x - \tfrac{1}{2}t_f w,_{xy})(\alpha_{fy}\psi,_y - \tfrac{1}{2}t_f w,_{yy})$$

$$+ \ 4c_f D_{26f}(\alpha_{fy}\psi,_x w,_{yy} - \tfrac{1}{2}t_f w,_{xy} w,_{yy}) \Big]$$

$$+ G_{xzc} t_c (\phi + w,_x)^2 + \frac{G_{yzc} t_c}{1 - \dfrac{\beta_1 \beta_2}{R_c^2}} (\psi + w,_y)^2$$

$$+ \lambda \left[N_{xf}^{(o)} w,_x^2 + 2 N_{xyf}^{(o)} w,_x w,_y \right] \Bigg\} dxdy \tag{2.17}$$

17

SECTION 3

DISCRETE FORMULATION

In this section the potential energy (Equation 2.17) is cast into a discrete form from which a numerical solution can be obtained for the buckling problem. The displacement field is expressed as a linear combination of known functions which satisfy the necessary conditions of kinematic admissibility. The corresponding discrete form of the potential energy is a quadratic function of a number of parameters: these are selected in such a manner that the energy expression is minimized.

3.1 DISCRETIZATION OF THE POTENTIAL ENERGY

The discrete counterpart of a functional $F[u(x, y)]$ is obtained by the introduction of an assumed-mode approximation of the form

$$u(x, y) = \sum_{j=1}^{N} c_j \chi_j(x, y), \tag{3.1}$$

where c_j; $j = 1, 2, \ldots, N$ are arbitrary constants, and $\chi_j(x, y)$ are known functions satisfying the imposed boundary conditions and appropriate requirements of continuity and differentiability.[27] For the displacement formulation, stress boundary conditions are satisfied as stationary conditions, while displacement boundary conditions are of the imposed type.[22] Thus, in the present problem, the assumed-mode approximations to the functions $\phi(x, y)$, $\psi(x, y)$ and $w(x, y)$ are required to satisfy the displacement conditions

$$\phi(x, o) = \phi(x, b) = 0$$

$$\psi(o, y) = \psi(a, y) = 0$$

$$w(x, o) = w(x, b) = 0 \tag{3.2}$$

$$w(o, y) = w(a, y) = 0.$$

The above boundary conditions correspond to simply-supported edges and vanishing core rotation on each boundary in the plane parallel to the panel

18

edges. A suitable approximation is therefore given by the functions

$$\phi(x, y) = \sum_{m=1}^{M_1} \sum_{n=1}^{N_1} \Phi_{mn} \cos\frac{m\pi x}{a} \sin\frac{n\pi y}{b}$$

$$\psi(x, y) = \sum_{m=1}^{M_1} \sum_{n=1}^{N_1} \Psi_{mn} \sin\frac{m\pi x}{a} \cos\frac{n\pi y}{b} \qquad (3.3)$$

$$w(x, y) = \sum_{m=1}^{M_2} \sum_{n=1}^{N_2} W_{mn} \sin\frac{m\pi x}{a} \sin\frac{n\pi y}{b}.$$

Introduction of Equations 3.3 into the potential energy (Equation 2.17) permits the direct evaluation of the integrations over the area, as described in Appendix B.

By inspection of Equation 2.17, it is evident that terms of the form $\alpha_{fx}^2 \Phi_{mn}^2$ will appear in the energy expression after the integrations have been performed. By Equation 2.5, such terms are of higher order than the desired quadratic, due to the dependence of α_{fx} and α_{fy} upon the neutral surface locations e_x and e_y. Recall that the parameters e_x and e_y, which are as yet undetermined, are dependent upon the displacement modes; that is,

$$e_x = e_x(m, n)$$

$$e_y = e_y(m, n)$$

The discretized energy expression can be reduced to the desired quadratic form by the use of the substitutions

$$h_{mn} = e_{xmn} \Phi_{mn}$$

$$k_{mn} = e_{ymn} \Psi_{mn}. \qquad (3.4)$$

An example of this substitution is given in Appendix B.

With these conventions, the potential energy is expressed in the matrix form

$$\pi_p = \frac{1}{2}\begin{Bmatrix} X_1 \\ X_2 \end{Bmatrix}^T \begin{bmatrix} A_{11} & A_{12} \\ A_{12}^T & A_{22} \end{bmatrix} \begin{Bmatrix} X_1 \\ X_2 \end{Bmatrix} + \frac{\lambda}{2}\begin{Bmatrix} X_1 \\ X_2 \end{Bmatrix}^T \begin{bmatrix} B_{11} & B_{12} \\ B_{12}^T & B_{22} \end{bmatrix} \begin{Bmatrix} X_1 \\ X_2 \end{Bmatrix}$$

$$(3.5)$$

19

The construction of the matrices of Equation 3.5 is described in Appendix C.

3.2 APPLICATION OF THE PRINCIPLE OF MINIMUM POTENTIAL ENERGY

The variational statement of the principle of minimum potential energy is expressed as

$$\delta \pi_p = 0. \tag{3.6}$$

The continuous displacement functions upon which π_p depends are in turn specified uniquely by the conditions of Equation 3.6. For the discrete, linear formulation, the potential energy $\bar{\pi}_p$ is a quadratic function of a number of undetermined coefficients (see Equation 3.1),

$$\bar{\pi}_p = \bar{\pi}_p(c_j; j = 1, 2, \ldots, N).$$

The coefficients are selected by requiring that the gradient of this function vanish:

$$\frac{\partial \bar{\pi}_p}{\partial c_j} = 0; \ j = 1, 2, \ldots, N. \tag{3.7}$$

For the present problem, the discretized potential energy (Equation 3.5) is to be minimized with respect to the components of the vectors $\{X_1\}$ and $\{X_2\}$. Thus it is required that

$$\left[\begin{array}{c|c} A_{11} & A_{12} \\ \hline A_{12}^T & A_{22} \end{array}\right] \left\{\begin{array}{c} X_1 \\ X_2 \end{array}\right\} + \lambda \left[\begin{array}{c|c} B_{11} & B_{12} \\ \hline B_{12}^T & B_{22} \end{array}\right] \left\{\begin{array}{c} X_1 \\ X_2 \end{array}\right\} = \left\{\begin{array}{c} 0 \\ 0 \end{array}\right\} \tag{3.8}$$

As noted in Appendix C, the matrices $[B_{11}]$ and $[B_{12}]$ are null matrices. Using this fact, Equation 3.8 can be restated as

$$[A_{11}]\{X_1\} + [A_{12}]\{X_2\} = 0 \tag{3.9}$$

$$[A_{12}]^T\{X_1\} + [A_{22}]\{X_2\} + \lambda[B_{22}]\{X_2\} = 0 \tag{3.10}$$

Combining Equations 3.9 and 3.10 yields

$$\{X_1\} = -[A_{11}]^{-1}[A_{12}]\{X_2\} \tag{3.11}$$

and

$$([A_{22}] - [A_{12}]^T[A_{11}]^{-1}[A_{12}])\{X_2\} + \lambda[B_{22}]\{X_2\}. \tag{3.12}$$

Equation 3.12 has the form of a generalized eigenvalue problem, which can be solved for the load intensity, λ, and the vector $\{X_2\}$ of transverse displacement modes. The remaining mode shape coefficients $\{X_1\}$ are then determined directly from Equation 3.11.

SECTION 4

NUMERICAL RESULTS

The numerical solution of Equations 3.11 and 3.12 is compared with a number of existing analytical results in this section to confirm its accuracy. Comparisons are made with experimental data, and the range of validity of the linear analysis procedure is discussed.

4.1 SOME COMMENTS ON THE NUMERICAL SOLUTION

In performing the numerical solution of Equations 3.11 and 3.12, the number of terms to be retained in the displacement functions (Equation 3.3) is generally dependent upon both the geometry of the panel and the type of loading to be considered. A panel having an aspect ratio which is significantly different from one, for example, may require a large number of terms for an adequate representation of the displacement state. Likewise, the presence of a shear load often dictates the use of a higher-order displacement approximation, since the deflected shape of the panel can be quite complex. For the results reported in this section, critical compression loads are calculated using $M_1 = N_1 = 3$ and $M_2 = N_2 = 6$ in Equation 3.3; solutions for critical shear loads or combined loads are based upon the limits of summation $M_1 = N_1 = 6$ and $M_2 = N_2 = 8$. The use of a greater number of terms in the series for the transverse deflection is motivated by the fact that this is the predominant mode of deformation; numerical experiments verify this fact. Furthermore, increasing the limits M_1 and N_1 has a significant effect on computation time, since the matrix $[A_{11}]$, which is to be inverted, is of the order $4M_1N_1$ (see Appendix C).

4.2 COMPARISON WITH ANALYTICAL RESULTS

Numerical solutions obtained by the present method are compared with previously published analytical results in Tables 1 to 3. Geometries considered include sandwich plates, laminated composite plates, and cylindrical shells of

22

both isotropic and sandwich construction.

Critical buckling loads calculated for flat sandwich panels are compared with previously reported results in Table 1. The first example is a square panel loaded in axial compression. The present analysis yields a value of the critical load which corresponds very closely with the nonlinear finite element result of Reference 28. The average experimental value obtained from four tests reported in Reference 32 is N_{xcr} = -283.3 lb./inch, indicating that both results are in error by about nine percent. The result of the present analysis corresponds exactly with that of Reference 21 for the second example of Table 1. This is to be expected, since the method of Reference 21 is a special case of the analysis described here. The effect of a reduced order of approximation for the core rotation functions (see paragraph 4.1) is illustrated by the last two problems considered in Table 1. The solution for a pure shear load using $M_1 = N_1 = 6$ and $M_2 = N_2 = 8$ with the present method agrees within one percent with the eight-term solution of Reference 21; for the final example, involving combined compression and shear, the difference in the two solutions is insignificant.

Table 2 summarizes the calculated values of critical loads for several orthotropic, laminated thin plates. The first two examples cited are taken from the nonlinear analysis of Reference 28. The comparison of the present results with those of the nonlinear analysis is very good. The second panel listed in Table 2 also shows close agreement with the experimental value N_{xcr} = -21.7 lb./inch reported in Reference 29. A thin plate subjected to a pure shear loading is the third example of Table 2. The calculated buckling load is in agreement with the five-term Ritz method solution of Reference 24.

Solutions for the critical loads of cylindrical shells of isotropic and sandwich construction are given in Table 3. The first case considered is that of an isotropic shell, analyzed by a linear method in Reference 30. The results correspond exactly in this instance. For the second problem, a sandwich shell loaded in axial compression is analyzed. A considerable improvement is observed over the results of Reference 19 in this case. An analysis

23

TABLE 1

SANDWICH PLATES -- COMPARISON WITH ANALYITICAL RESULTS

	1	2	3	4
E_f	9.5×10^6	10.6×10^6	10.6×10^6	9.5×10^6
ν_f	.30	.30	.25	.30
t_f	.021	.025	.025	.021
G_{xzc}	19000.	50000.	4359.	19000.
G_{yzc}	19000.	20000.	4359.	19000.
t_c	.181	.25	.25	.181
a	23.5	60.	10.	20.
b	23.5	20.	40.	20.
Loading	Compression	Compression	Shear	Compression and Shear*
Reference	28	21	21	21
Reference Result	-307.5	-1025.7	±1344.3	$N_x = -411.5$ $N_{xy} = \pm137.2$
Present Analysis	-309.4	-1025.7	±1374.1	$N_x = -411.8$ $N_{xy} = \pm137.3$

*such that $N_x = 3N_{xy}$

TABLE 2

THIN LAMINATED PLATES -- COMPARISON WITH
ANALYTICAL RESULTS

	1	2	3
A_{11}	1.021×10^6	3.118×10^5	3.027×10^6
A_{12}	$.850 \times 10^6$	$.177 \times 10^5$	$.091 \times 10^6$
A_{22}	1.021×10^6	3.118×10^5	$.303 \times 10^6$
A_{66}	$.862 \times 10^6$	$.273 \times 10^5$	$.207 \times 10^6$
D_{11}	1.011×10^6	127.	2.523×10^3
D_{12}	$.842 \times 10^6$	4.45	$.076 \times 10^3$
D_{22}	1.011×10^3	30.2	$.252 \times 10^3$
D_{66}	$.854 \times 10^3$	6.88	$.173 \times 10^3$
t	.109	.055	.100
a	11.	10.	20.
b	9.75	10.	20.
Loading	Compression	Compression	Shear
Reference	28	28	24
Reference Result	-745	-19.2	±194.9
Present Analysis	-745.6	-19.1	±195.0

25

identical to that of Reference 19, but neglecting the flexural stiffnesses of the face sheets, is presented in Reference 33. By that method, a value of N_{xcr} = -760 lb./inch is obtained for the second case of Table 3. The last example considered, a cylindrical sandwich shell loaded in shear, corresponds almost exactly with the numerical value given in Reference 16. However, an experimental result of N_{xycr} = 227 lb./inch, reported in Reference 31, suggests that the numerical solution is grossly in error. This discrepancy is due in part to the depth of the shell, as discussed in the following sections, and to difficulties which are typically encountered in experimentally maintaining a true simply-supported boundary condition in the presence of a uniform shear load.

4.3 COMPARISON WITH EXPERIMENTAL DATA

The present analysis has been used to predict the critical loads of cylindrical panels in axial compression for a number of known experimental cases.[13, 34] A comparison of the analytical and experimental results is summarized in this section.
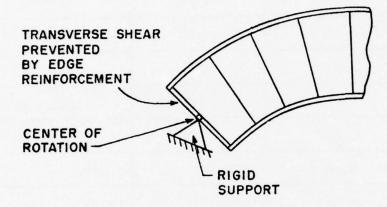
An important comment is necessary concerning the effects of differences between the theoretical and experimental boundary conditions, and the implications of the present choice of assumed mode functions. In the experimental studies reported in References 13 and 34, the loaded edges of the specimens were attached to metal strips, while the unloaded edges were supported only by loose-fitting wooden guides slipped onto the edges. Such a method of support resembles the theoretical simple support provided the included angle of the panel is small. However, for very deep panels, it appears that the experimental edge condition is more flexible than the theoretical support condition, since the analysis boundary condition imposes a rigid reaction in the direction exactly normal to the panel. Both boundary conditions are pictured schematically in Figure 3. In addition to this apparent discrepancy in the boundary conditions, it is important to note that the assumed mode functions (Equation 3.3) employed in the analysis are periodic with respect to the

TABLE 3

CYLINDRICAL SHELLS -- COMPARISON WITH
ANALYTICAL RESULTS

E_{xf}	1×10^7	1×10^7	4.19×10^6
E_{yf}	1×10^7	1×10^7	4.01×10^6
ν_{xyf}	.30	.30	.150
G_{xyf}	$.385 \times 10^7$	$.385 \times 10^7$	$.562 \times 10^6$
t_f	.020*	.010	.021
G_{xzc}	N. A. **	10000.	32000.
G_{yzc}	N. A.	10000.	18300.
t_c	N. A.	.1875	.300
R	50.	50.	21.94
Θ	34.4^o	34.4^o	$128.^o$
a	30.	30.	49.
b	30.	30.	49.
Loading	Compression	Compression	Shear
Reference	30	19	16
Reference Result	-81.0	-823.	±630.
Present Analysis	-81.0	-773.	±629.

*Total thickness of isotropic shell
**Not Applicable

27

IDEALIZED SIMPLE SUPPORT

TRANSVERSE SHEAR
PREVENTED
BY EDGE
REINFORCEMENT

CENTER OF
ROTATION

RIGID
SUPPORT

TYPICAL EXPERIMENTAL SUPPORT

POSSIBLE
CENTERS OF
ROTATION

WOODEN
GUIDE
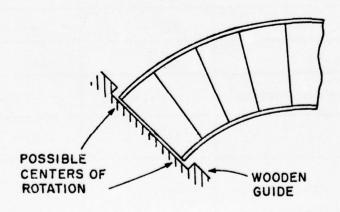
Figure 3

Comparison of Theoretical and Experimental Boundary
Conditions

28

circumferential dimension of the panel, so that the trial space of functions disallows the accurate representation of deformations which are axisymmetric in nature. As the included angle of the panel becomes large, the buckling deflections can be expected to approach the *axisymmetric deformations* which are typical of a full cylinder. For these reasons, the present analysis should be expected to yield accurate results only for panels which are sufficiently shallow that the form of the assumed mode approximations and the chosen boundary conditions are appropriate.

The test data of Reference 34 are given in Table 4, with the corresponding numerical results obtained by the present analysis. Each of the experimental specimens has aluminum face sheets, ranging between .005 inch and .032 inch in thickness, bonded to an end-grain balsa core having a nominal thickness of .125 inch[*]. The core shear moduli used for the calculations are based upon average moduli [35] for the *density range of the experimental core* material, and therefore are not exact. However, numerical experimentation shows that an increase in the core modulus by as much as a factor of three produces an increase in the calculated critical load which is on the order of one percent. The lack of precise data for the core moduli is therefore not expected to be critical to the comparison of numerical and experimental buckling loads.

The comparison of analytical and experimental results in Table 4 indicates reasonably good agreement for panels having small included angles. Relative errors in the calculated values range from 4.5% (for $\Theta = 14^{\circ}$) to more than 175% (for $\Theta = 42.9^{\circ}$). Furthermore, the least errors, for panels having large *included angles*, are observed for those panels having the smallest overall surface dimensions. This trend is significant in that the influence of the experimental boundary conditions is indicated, since the smaller panels are better represented by the theory.

---

[*]Exact dimensions for each of the specimens are tabulated in Reference 34.

29

TABLE 4

COMPARISON OF ANALYTICAL VALUES WITH EXPERIMENTAL DATA OF REFERENCE 34.

Specimen No.	Length a (in.)	Radius R_c (in.)	Angle Θ (deg.)	N_{xcr} (exptl.)	N_{xcr} (calc.)
55-1	29.0	63.2	17.4	-165.	-229.
55-2	29.0	63.2	17.3	-183.	-231.
56-1	28.9	59.9	14.0	-220.	-230.
56-2	28.9	63.2	13.2	-200.	-220.
58-1	41.1	51.0	46.3	-473.	-687.
58-2	41.0	48.3	48.9	-430.	-735.
58-3	41.0	51.7	45.8	-487.	-699.
60-2	59.9	77.4	42.9	-518.	-1432.
61-1	70.0	92.9	42.7	-170.	-419.
61-2	59.9	104.0	32.6	-199.	-353.
61-3	69.9	73.2	54.2	-199.	-484.

All specimens Aluminum faces on balsa wood core.

$E_f = 10. \times 10^6$ psi, $\nu_f = .30$, $G_c \approx 10000.$ psi

The experimental data reported in Reference 13 have also been studied by the present analysis method. The test specimens are constructed of aluminum face sheets, between .012 inch and .032 inch in thickness, bonded to corkboard cores. Pertinent geometrical data are given with the comparisons of critical loads in Table 5. The relative errors in the calculated buckling loads are seen to be quite poor for this group of specimens.

One important difference exists between the two sets of test specimens described above. For the panels described in Reference 34 the core shear moduli are approximately 10,000 psi based on average values taken from Reference 35. The moduli of the test specimens reported in Reference 13 are between 320 and 15,000 psi, but fall primarily in the range 320 - 1000 psi. Thus, the analysis procedure is more accurate when the shear rigidity of the sandwich core is relatively large.

The relative errors observed for numerically determined buckling loads in axial compression are plotted versus panel included angle in Figure 4. This data includes the cylindrical panels from References 13 and 34, and two flat panels (see paragraph 4.1) cited from References 29 and 32. A number of conclusions can be made from this plot:
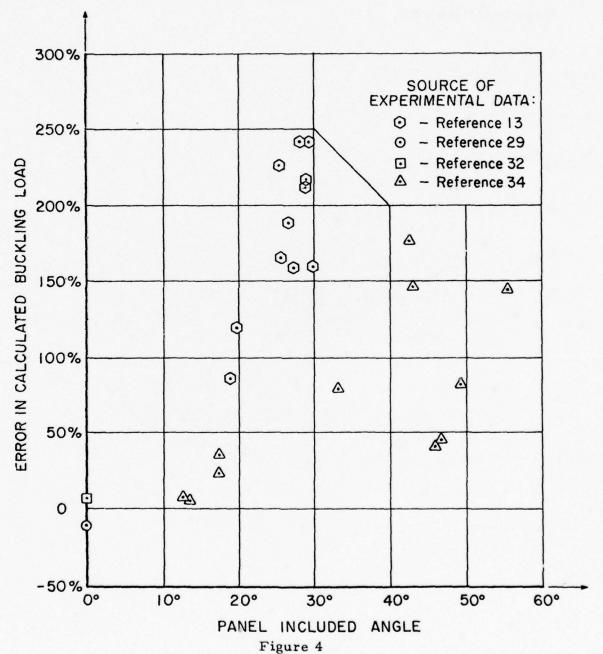
1. For panels having very mild curvature (included angles of approximately 15° or less), the linear buckling analysis gives reliable results in most instances. The error committed in the linear analysis tends to increase very rapidly past this limit, however. A similar limitation is reported[30] for isotropic shells, for included angles larger than about 30°.

2. The error in the numerical solution is the most serious for sandwich panels having relatively weak cores. This suggests that the prebuckling deformation may be more significant for weak-core sandwich, or that the adoption of a linear displacement field through the core thickness is unduly restrictive for such problems.

31

TABLE 5

COMPARISON OF ANALYTICAL VALUES WITH EXPERIMENTAL
DATA OF REFERENCE 13

Specimen No.	Length a (in.)	Radius R_c (in.)	Angle Θ (deg.)	N_{xcr} (exptl.)	N_{xcr} (calc.)
9114-17	29.9	23.8	29.2	-373.	-1186.
61-1	70.0	92.9	43.0	-170.	-421.
61-3	69.9	73.2	54.4	-199.	-486.
1155-10	30.0	24.4	28.6	-466.	-1467.
9114-10	29.7	26.2	26.4	-267.	-773.
1463-25	29.4	22.9	29.8	-779.	-2652.
1155-25	29.9	23.2	29.8	-776.	-2024.
9114-25	29.8	27.2	25.2	-479.	-1096.
1155-6	29.9	60.5	18.9	-255.	-475.
1463-3	29.4	23.6	28.6	-384.	-1305.
1155-3	29.9	27.7	25.2	-289.	-942.
9114-6	29.8	58.6	19.5	-132.	-292.
9114-3	30.0	26.0	26.9	-225.	-586.

Figure 4

Error in Theoretical Buckling Load versus Panel Included
Angle

3. Scatter observed in the experimental values increases rapidly with the panel included angle. This fact supports the previous comments regarding degeneration of the experimental boundary conditions for large included angles.

SECTION 5

SUMMARY AND CONCLUSIONS

A method of analysis has been presented for the prediction of stability of open cylindrical sandwich shells subjected to axial compression and shear loading. The mathematical model is obtained from the linearized principle of minimum potential energy. The total potential energy, consisting of internal elastic strain energy and applied loads potentials, is formulated in terms of displacements within the core of the sandwich. The Ritz method is used to transform the resulting functional into a quadratic function of a set of discrete parameters, which are then selected in such a way that the energy is a minimum. The infinite sequences of eigenvalue and eigenfunctions for the continuous problem are approximated by the finite number of eigenvalues and eigenvectors thus obtained, the lowest eigenvalue corresponding to the load intensity for which instability is first observed.

The analysis method described has been compared with numerous existing results, both theoretical and experimental. Agreement with the experimental results is shown to vary in a somewhat predictable pattern as a function of the included angle of the panel, and to be influenced by both the overall panel dimensions and the shear rigidity of the core. At least some of the disagreement between theory and experiment can be attributed to the variation in experimental edge conditions, although further study is required in order to evaluate the effect accurately. A few theoretical values obtained for shallow panels with relatively strong cores are encouraging, showing relative errors of five to ten percent based on test data.

The present study has demonstrated that while the linear theory of sandwich shell stability is restricted to a rather small class of geometric configurations, it is possible to obtain useful results by respecting the limitations of the theory. For deep shell geometries, it is evident that a more sophisticated analysis, incorporating the effects of prebuckling deformation, is required. Further study will help to define the limitations of the linear formulation with greater clarity.

35

REFERENCES

1. Habip, L. M., "A Survey of Modern Developments in the Analysis of Sandwich Structures," Applied Mechanics Review, Vol. 18, No. 2, 1965.

2. Graziano, E. E., "All-metal Sandwiches except Honeycomb--An Annotated Bibliography," Report 3-77-62-5/SB-62-8, Lockheed Aircraft Corp., Sunnyvale, CA., ASTIA AD275280, 1962.

3. Foss, J. U., "For the Space Age, A Bibliography of Sandwich Plates and Shells," Report SM-42883, Douglas Aircraft Co., Santa Monica, CA., 1962.

4. Bert, C. W., and P. H. Francis, "Composite Material Mechanics: Structural Mechanics," AIAA Journal, Vol. 12, No. 9, 1974.

5. March, H. W., "Effects of Shear Deformation in the Core of a Flat, Rectangular Sandwich Panel," Forest Products Laboratory Report 1583, 1948.

6. Hoff, N. J., "Bending and Buckling of Rectangular Sandwich Plates," NACA TN2225, 1950.

7. March N. W., and C. B. Smith, "Buckling loads of Flat Sandwich Panels in Compression--Various Types of Edge Conditions," Forest Products Laboratory Report 1525, 1945.

8. Kuenzi, E. W., W. S. Ericksen and J. J. Zahn, "Shear Stability of Flat Panels of Sandwich Construction," Forest Products Laboratory Report 1560, Revised 1962.

9. Allen, H. G., Analysis and Design of Structural Sandwich Panels, Pergamon Press, 1969.

36

10.   Kimel, W. R., "Elastic Buckling of a Simply-Supported Rectangular
          Sandwich Panel Subjected to Combined Edgewise Bending
          and Compression," Forest Products Laboratory Report
          1857, 1956.

11.   Baker, E. H., "Stability of Circumferentially Corrugated Sandwich
          Cylinders under combined loads," AIAA Journal, Vol. 2,
          No. 12, 1964.

12.   Teichmann, F. K., C. T. Wang and G. Gerard, "Buckling of Sandwich
          Cylinders under Axial Compression," Journal of the
          Aeronautical Sciences, Vol. 18, June, 1951.

13.   March, H. W., and E. W. Kuenzi, "Buckling of Cylinders of Sandwich
          Construction in Axial Compression," Forest Products
          Laboratory Report 1830, Revised 1957.

14.   Norris, C. B., and J. J. Zahn, "Compressive Buckling Curves for
          Sandwich Cylinders having Orthotropic Facings," Forest
          Products Laboratory Report 1876, July 1960.

15.   Bartelds, G., and J. Mayers, "Unified Theory for the Bending and
          Buckling of Sandwich Shells--Application to Axially
          Compressed Circular Cylindrical Shells," SUDAAR 287,
          Stanford University, 1966.

16.   Davenport, O. B., "Buckling of Orthotropic, Curved Sandwich Panels
          Subjected to Edge Shear and Axial Compression," M. S.
          Thesis, Department of Aerospace, Mechanical and Nuclear
          Engineering, University of Oklahoma, 1972.

17.   Stein, M., and J. Mayers, "A Small-Deflection Theory for Curved
          Sandwich Plates," NACA Report 1008, 1951.

18.   Pope, G. G., "The Buckling Behavior in Axial Compression of Slightly-
          Curved Panels, including the Effects of Shear Deformability,"
          International Journal of Solids and Structures, Vol. 4,
          No. 3, 1968.

19. Fulton, R. E., "Effect of Face-Sheet stiffness on Buckling of Curved Plates and Cylindrical Shells of Sandwich Construction in Axial Compression," NASA TN-D-2783, 1965.

20. Bogner, F. K., "Theory of Sandwich Plates," University of Dayton Research Institute, UDRI-TR-76-01, 1976.

21. Brockman, R. A., "Stability of Flat, Simply Supported, Rectangular Sandwich Panels Subjected to Combined Inplane Loadings," AFFDL-TR-76-14, Air Force Flight Dynamics Laboratory, Wright-Patterson Air Force Base, Dayton, Ohio, 1976.

22. Washizu, K., Variational Methods in Elasticity and Plasticity, Pergamon Press, 1968.

23. Novozhilov, V. V., Thin Shell Theory, Second Revised Edition, P. G. Lowe, Translator, J. R. M. Radok, Ed., Wolters-Noordhoff Publishing, Groningen, the Netherlands, 1970.

24. Ashton, J. E., and J. M. Whitney, Theory of Laminated Plates, Technomic Publishing Co., Stamford, Conn., 1970.

25. Reissner, E., and Y. Stavsky, "Bending and Stretching of Certain Types Heterogeneous Aelotropic Elastic Plates," Trans. ASME, Journal of Applied Mechanics, Vol. 28, No. 3, 1961.

26. Ashton, J. E., J. C. Halpin, and P. H. Petit, Primer on Composite Materials: Analysis, Technomic Publishing Co., Stamford, Conn., 1969.

27. Crandall, S. H., Engineering Analysis, McGraw-Hill Publishing Co., 1956.

28. Monoforton, G. R., "Discrete Element Finite Displacement Analysis of Anisotropic Sandwich Shells," Report No. 39, Department of Solid Mechanics, Structures and Mechanical Design, Case Western Reserve University, 1970.

29. Mandell, J. F., "An Experimental Study of the Buckling of Anisotropic
    Plates," AFML-TR-68-281, Air Force Materials
    Laboratory, Wright-Patterson Air Force Base, Dayton,
    Ohio, 1968.

30. Timoshenko, S. P., and J. M. Gere, Theory of Elastic Stability,
    2nd Edition, McGraw Hill Publishing Co., 1961.

31. Bert, C. W., W. C. Crisman and G. M. Nordby, "Fabrication and
    Full-scale Evaluation of Glass-Fabric Reinforced Plastic
    Shells," Journal of Aircraft, Vol. 5, No. 1, Jan.-Feb. 1968.

32. Boller, K. H., "Buckling Loads of Flat Sandwich Panels in Compression,"
    Forest Products Laboratory Report 1525A, 1954.

33. Stein, M., and J. Mayers, "Compressive Buckling of Simply-Supported
    Curved Plates and Cylinders of Sandwich Construction"
    NACA TN2601, 1952.

34. Kuenzi, E. W., "Design Criteria for long Curved Panels of Sandwich
    Construction in Axial Compression," Forest Products
    Laboratory Report 1558, 1946.

35. Doyle, D. V., J. T. Drow and R. S. McBurney, "Elastic Properties of
    Wood," Forest Products Laboratory Report 1528, 1956.

APPENDIX A

STIFFNESS PARAMETERS FOR A LAMINATED FACE SHEET

The present formulation of stress-strain equations for the sandwich face sheets follows the derivation presented in Reference 24. Each of the face sheets is treated as a thin shell composed of arbitrarily oriented layers, subject to the Love-Kirchhoff assumptions. Each individual layer is of uniform thickness and obeys the generalized Hooke's law equations.

Let (x, y) denote the structural coordinate lines of the face sheet, and $(1, 2)$ represent the principal orthotropic axes of a layer within the sheet. The stress-strain equations for layer k of face f are given by [24]

$$
\begin{Bmatrix} \sigma_{1f}^k \\[6pt] \sigma_{2f}^k \\[6pt] \tau_{12f}^k \end{Bmatrix} = \begin{bmatrix} C_{11f}^k & C_{12f}^k & 0 \\[6pt] C_{12f}^k & C_{22f}^k & 0 \\[6pt] 0 & 0 & C_{66f}^k \end{bmatrix} \begin{Bmatrix} \epsilon_{1f}^k \\[6pt] \epsilon_{2f}^k \\[6pt] \gamma_{12f}^k \end{Bmatrix} \tag{A1}
$$

where

$$
C_{11f}^k = E_{11f}^k / (1 - \nu_{12f}^k \nu_{21f}^k)
$$

$$
C_{12f}^k = \nu_{12f}^k E_{22f}^k / (1 - \nu_{12f}^k \nu_{21f}^k)
$$

$$
C_{22f}^k = E_{22f}^k / (1 - \nu_{12f}^k \nu_{21f}^k)
$$

$$
C_{66f}^k = G_{12f}^k.
$$

Let the angle separating the coordinates (x, y) and $(1, 2)$ be θ, and define

$$
m = \cos\theta
$$

$$
n = \sin\theta
$$

A transformation of the stiffness properties to the (x, y) coordinate system gives

$$\left\{ \begin{matrix} \sigma_{xf}^{k} \\ \sigma_{yf}^{k} \\ \tau_{xyf}^{k} \end{matrix} \right\} = \left[\begin{matrix} Q_{11f}^{k} & Q_{12f}^{k} & Q_{16f}^{k} \\ Q_{22f}^{k} & Q_{22f}^{k} & Q_{26f}^{k} \\ Q_{16f}^{k} & Q_{26f}^{k} & Q_{66f}^{k} \end{matrix} \right] \left\{ \begin{matrix} \epsilon_{xf}^{k} \\ \epsilon_{yf}^{k} \\ \gamma_{xyf}^{k} \end{matrix} \right\} \tag{A2}$$

where

$$\left\{ \begin{matrix} Q_{11f}^{k} \\ Q_{12f}^{k} \\ Q_{16f}^{k} \\ Q_{22f}^{k} \\ Q_{26f}^{k} \\ Q_{66f}^{k} \end{matrix} \right\} = \left[\begin{matrix} m^{4} & 2m^{2}n^{2} & n^{4} & 4m^{2}n^{2} \\ m^{2}n^{2} & (m^{4} + n^{4}) & m^{2}n^{2} & -4m^{2}n^{2} \\ -m^{3}n & mn(m^{2} - n^{2}) & mn^{3} & 2mn(m^{2} - n^{2}) \\ n^{4} & 2m^{2}n^{2} & m^{4} & 4m^{2}n^{2} \\ -mn^{3} & mn(n^{2} - m^{2}) & m^{3}n & 2mn(n^{2} - m^{2}) \\ m^{2}n^{2} & -2m^{2}n^{2} & m^{2}n^{2} & (m^{2} - n^{2})^{2} \end{matrix} \right] \left\{ \begin{matrix} c_{11f}^{k} \\ c_{12f}^{k} \\ c_{22f}^{k} \\ c_{66f}^{k} \end{matrix} \right\}.$$

Thus, Equation A2 relates the stresses and strains, referred to the structural axes of the shell, in layer k of the face sheet.

By Equation 2.11, the strains are separated into uniform and linearly-varying components,

$$\left\{ \begin{matrix} \epsilon_{xf}^{k} \\ \epsilon_{yf}^{k} \\ \gamma_{xyf}^{k} \end{matrix} \right\} = \left\{ \begin{matrix} \epsilon_{xf}^{o} \\ \epsilon_{yf}^{o} \\ \gamma_{xyf}^{o} \end{matrix} \right\} + z_{f} \left\{ \begin{matrix} \varkappa_{xf} \\ \varkappa_{yf} \\ \varkappa_{xyf} \end{matrix} \right\}, \tag{A3}$$

where z_{f} is the distance from the midsurface of the face. The result of combining Equations A2 and A3 is written symbolically as

$$\left\{ \sigma_{f}^{k} \right\} = \left[Q_{f}^{k} \right] \left[\left\{ \epsilon_{f}^{o} \right\} + z_{f} \left\{ \varkappa_{f} \right\} \right]. \tag{A4}$$

41

The stress and moment resultants for the face sheet are defined to be

$$(N_{xf}, \ N_{yf}, \ N_{xyf}) = \int_{-t_{f/2}}^{t_{f/2}} (\sigma_{xf}^{k}, \ \sigma_{yf}^{k}, \ \tau_{xyf}^{k}) dz_f$$

$$\text{(A5)}$$

$$(M_{xf}, \ M_{yf}, \ M_{xyf}) = \int_{-t_{f/2}}^{t_{f/2}} (\sigma_{xf}^{k}, \ \sigma_{yf}^{k}, \ \tau_{xyf}^{k}) z_f dz_f,$$

where the superscript k refers to the particular layer at a station z_f within the integration. Integration of Equation A4 through the thickness with respect to weighting functions 1 and z_f yields

$$\left\{ \frac{N_f}{M_f} \right\} = \left[\begin{array}{c|c} A_f & B_f \\ \hline B_f & D_f \end{array} \right] \left\{ \frac{\varepsilon_f^o}{\varkappa_f} \right\}. \qquad \text{(A6)}$$

The elements of the 3x3 symmetric matrices A_f, B_f and D_f are defined by

$$(A_{ijf}, \ B_{ijf}, \ D_{ijf}) = \int_{t_{f/2}}^{t_{f/2}} (1, \ z_f, \ z_f^2) Q_{ijf} dz_f; \ i, \ j = 1, \ 2, \ 6 \qquad \text{(A7)}$$

By Equations A6 and A7, the membrane stress resultants and moment resultants are related to the midsurface strains and curvatures in a simple, concise manner.

APPENDIX B

INTEGRATION FORMULAS

The following formulas are used in performing the area integrations of the discretized potential energy function:

$$\int_o^a \sin\frac{i\pi x}{a} \sin\frac{j\pi x}{a} dx = \frac{a}{2}\delta_{ij}$$

$$\int_o^a \cos\frac{i\pi x}{a} \cos\frac{j\pi x}{a} dx = \frac{a}{2}\delta_{ij} \tag{B1}$$

$$\int_o^a \sin\frac{i\pi x}{a} \cos\frac{j\pi x}{a} dx = \frac{2ai}{\pi(i^2 - j^2)} \Delta_{ij}$$

$$\int_o^a \cos\frac{i\pi x}{a} \sin\frac{j\pi x}{a} dx = \frac{2aj}{\pi(j^2 - i^2)} \Delta_{ij}$$

Here i and j are integer indices, and δ_{ij} is the Kronecker delta,

$$\delta_{ij} = \begin{cases} 1 \; ; \; i = j \\ 0 \; ; \; i \neq j. \end{cases} \tag{B2}$$

The operator Δ_{ij} is defined in such a way that, for any algebraic function X,

$$X\Delta_{ij} = \begin{cases} X \; ; \; i + j \; \text{odd} \\ o \; ; \; i + j \; \text{even.} \end{cases} \tag{B3}$$

The above definition is understood to apply also to the case where the function X is indefinite, as for i = j in the last two integrals of Equation B1.

The mechanics of performing the integrations is best illustrated by a simple example. Consider the first term of the potential energy (Equation 2.17),

$$T_1 = \sum_{f=1}^2 \int_o^{b_f} \int_o^a \frac{1}{2} A_{11f} \, \alpha_{fx}^2 \, \phi_{,x}^2 \, dxdy.$$

Substituting the assumed mode approximation (Equation 3.3) gives

43

$$T_1 = \sum_{f=1}^{2} \int_{o}^{b_f} \int_{o}^{a} \frac{1}{2} A_{11f} \sum_{m=1}^{M_1} \sum_{n=1}^{N_1} \frac{m\pi}{a} \Phi_{mn} \sin\frac{m\pi x}{a} \sin\frac{n\pi y}{b} \; X$$

$$\sum_{r=1}^{M_1} \sum_{s=1}^{N_1} \frac{r\pi}{a} \Phi_{rs} \sin\frac{r\pi x}{a} \sin\frac{n\pi y}{b} \; \alpha_{fx}^2 \; dxdy,$$

or, rearranging this,

$$T_1 = \sum_{f=1}^{2} \frac{1}{2} A_{11f} \sum_{m=1}^{M_1} \sum_{r=1}^{M_1} \int_{o}^{a} \sin\frac{m\pi x}{a} \sin\frac{r\pi x}{a} dx \sum_{n=1}^{N_1} \sum_{s=1}^{N_1} \int_{o}^{b_f} \; X$$

$$\sin\frac{n\pi y}{b} \sin\frac{s\pi y}{b} \; dy \frac{mr\pi^2}{a^2} \alpha_{fx}^2 \Phi_{mn} \Phi_{rs}.$$

Next, the integrations are performed according to Equation B1. Using Equations B2 and B3, the resulting expression is

$$T_1 = \sum_{f=1}^{2} \frac{1}{2} A_{11f} \sum_{m=1}^{M_1} \sum_{n=1}^{N_1} \frac{m^2 \pi^2 b_f}{4_a} \alpha_{fx}^2 \Phi_{mn}^2.$$

Substituting for α_{fx} from Equation 2.5, one obtains

$$T_1 = \sum_{f=1}^{2} \frac{1}{2} A_{11f} \sum_{m=1}^{M_1} \sum_{n=1}^{N_1} \frac{m^2 \pi^2 b_f}{4_a} (\beta_f^2 \Phi_{mn}^2 + 2c_f \beta_f e_{xmn} + e_{xmn}^2) \Phi_{mn}^2.$$

It should be noted that the terms $e_{xmn} \Phi_{mn}^2$ and $e_{xmn}^2 \Phi_{mn}^2$ are expressions of cubic and quartic order, respectively, for reasons described in Paragraph 3.1. Using the definition for h_{mn} (Equation 3.4), terms of the desired quadratic order are obtained:

44

$$T_1 = \sum_{f=1}^{2} \frac{1}{2} A_{11f} \sum_{m=1}^{M_1} \sum_{n=1}^{N_1} \frac{m^2 \pi^2 b_f}{4_a} \left[\beta_f^2 \Phi_{mn}^2 + 2c_f \beta_f \Phi_{mn} h_{mn} + h_{mn}^2 \right] .$$

The collection of the above and similar expressions into a convenient matrix form is outlined in Appendix C.

APPENDIX C

STIFFNESS AND GEOMETRIC MATRIX FORMULAS

Definitions are made in this Appendix for the entries of the elastic and geometric stiffness matrices of Equation 3.5. The symbols δ_{ij} and Δ_{ij} are used as defined in Appendix B. The following notational convention is also extablished: The superscript T, when assigned to an expression $F(i, j, k, 1,)$ is taken to mean

$$F^T(i, j, k, 1) = F(k, 1, i, j),$$

where i, j, k and l are integer indices.

The assumed-mode coefficients (Equation 3.3) are arranged in order in the vectors

$$\{\Phi\}^T = \left\lfloor \Phi_{11}, \Phi_{12}, \ldots \Phi_{1N_1}, \Phi_{21}, \ldots \ldots \Phi_{M_1N_1} \right\rfloor$$

$$\{\Psi\}^T = \left\lfloor \Psi_{11}, \Psi_{12}, \ldots \Psi_{1N_1}, \Psi_{21}, \ldots \ldots \Psi_{M_1N_1} \right\rfloor$$

$$\{h\}^T = \left\lfloor h_{11}, h_{12}, \ldots h_{1N_1}, h_{21}, \ldots \ldots h_{M_1N_1} \right\rfloor \tag{C1}$$

$$\{k\}^T = \left\lfloor k_{11}, k_{12}, \ldots k_{1N_1}, k_{21}, \ldots \ldots k_{M_1N_1} \right\rfloor$$

$$\{w\}^T = \left\lfloor w_{11}, w_{12}, \ldots w_{1N_2}, w_{21}, \ldots \ldots w_{M_2N_2} \right\rfloor.$$

The assembled vectors of unknowns (Equation 3.5) are then defined as

$$\{X_1\} = \begin{bmatrix} \{\Phi\} \\ \{\Psi\} \\ \{h\} \\ \{k\} \end{bmatrix}, \qquad \{X_2\} = \{w\}. \tag{C2}$$

46

Note that the dimension of $\{X_1\}$ is $4\,M_1 N_1$, and that of $\{X_2\}$ is $M_2 N_2$.

The elastic stiffness matrix is defined by

$$[A] = \begin{bmatrix} A^{11} & A^{12} & A^{13} & A^{14} & \bigm| & A^{15} \\ & A^{22} & A^{23} & A^{24} & \bigm| & A^{25} \\ & & A^{33} & A^{34} & \bigm| & A^{35} \\ & & & A^{44} & \bigm| & A^{45} \\ & & & & \bigm| & \\ \underline{\text{symmetric}} & & & & \bigm| & \\ & & & & \bigm| & A^{55} \end{bmatrix} , \qquad (C3)$$

where the numbering A^{ij} refers to the ordering of the vectors of assumed-mode parameters within $\{X_1\}$ and $\{X_2\}$. For example, A^{13} is the submatrix obtained from the products of $\Phi_{mn} h_{rs}$ in the potential energy expression. The individual entries A_{ij}^{kl} of the submatrix A^{kl} are given by

$$a_{ij}^{11} = \sum_{f=1}^{2} \beta_f^2 H_{1f}(m, n, r, s) + G_{xzc} t_c \frac{ab_c}{4} \delta_{mr} \delta_{ns}$$

$$a_{ij}^{12} = \sum_{f=1}^{2} \beta_f^2 H_{3f}(m, n, r, s)$$

$$a_{ij}^{13} = \sum_{f=1}^{2} C_f \beta_f H_{1f}(m, n, r, s)$$

$$a_{ij}^{14} = \sum_{f=1}^{2} C_f \beta_f H_{3f}(m, n, r, s)$$

$$a_{ij}^{15} = -\sum_{f=1}^{2} \beta_f H_{5f}(m, n, r, s) + G_{xzc} t_c \frac{m\pi b_c}{4} \delta_{mr} \delta_{ns}$$

47

$$a_{ij}^{22} = \sum_{f=1}^{2} \beta_f^2 H_{2f}(m, n, r, s) + G_{yzc} t_c \frac{ab_c}{4} \delta_{mr}\delta_{ns}$$

$$a_{ij}^{23} = \sum_{f=1}^{2} C_f \beta_f H_{4f}(m, n, r, s)$$

$$a_{ij}^{24} = \sum_{f=1}^{2} C_f \beta_f H_{2f}(m, n, r, s)$$

$$a_{ij}^{25} = -\sum_{f=1}^{2} \beta_f H_{7f}(m, n, r, s) + G_{yzc} t_c \frac{n\pi a}{4} \delta_{mr}\delta_{ns}$$

$$a_{ij}^{33} = \sum_{f=1}^{2} H_{1f}(m, n, r, s)$$

$$a_{ij}^{34} = \sum_{f=1}^{2} H_{3f}(m, n, r, s)$$

$$a_{ij}^{35} = -\sum_{f=1}^{2} c_f H_{5f}(m, n, r, s)$$

$$a_{ij}^{44} = \sum_{f=1}^{2} H_{2f}(m, n, r, s)$$

$$a_{ij}^{45} = -\sum_{f=1}^{2} c_f H_{7f}(m, n, r, s)$$

$$a_{ij}^{55} = \sum_{f=1}^{2} H_{9f}(m, n, r, s) + \left(G_{xzc} t_c \frac{m^2}{a^2} + G_{yzc} t_c \frac{n^2}{b_c^2} \right) \frac{\pi^2 ab_c}{4} \delta_{mr}\delta_{ns}, \quad \text{(C4)}$$

where the following definitions are used:

$$H_{1f}(m, n, r, s) = \left(A_{11f} \frac{m^2 \pi^2 b_f}{4_a} + A_{66f} \frac{n^2 \pi^2 a}{46_f} \right) \delta_{mr} \delta_{ns}$$

$$- 4A_{16f} \frac{(m^2 + r^2)ns}{(m^2 - r^2)(n^2 - s^2)} \Delta_{mr} \Delta_{ns}$$

$$H_{2f}(m, n, r, s) = \left[\left(A_{22f} + 2\frac{B_{22f}}{R_f} + \frac{D_{22f}}{R_f^2} \right) \frac{n^2 \pi^2 a}{4b_f} \right.$$

$$\left. + \left(A_{66f} + 4\frac{B_{66f}}{R_f} + 4\frac{D_{66f}}{R_f^2} \right) \frac{m^2 \pi^2 b_f}{4a} \right] \delta_{mr} \delta_{ns}$$

$$H_{3f}(m, n, r, s) = \left[A_{12f} + A_{66f} + \frac{1}{R_f}(B_{12f} + 2B_{66f}) \right] \frac{mn\pi^2}{4} \delta_{mr} \delta_{ns}$$

$$- 4 \left[\left(A_{16f} + 2\frac{B_{16f}}{R_f} \right) \frac{m^2}{a^2} + \left(A_{26f} + \frac{B_{26f}}{R_f} \right) \frac{s^2}{b_f^2} \right] \frac{nrab_f}{(m^2 - r^2)(n^2 - s^2)} \Delta_{mr} \Delta_{ns}$$

$$H_{4f}(m, n, r, s) = H_{3f}^{T}(m, n, r, s)$$

$$H_{5f}(m, n, r, s) = \left[-A_{12f} \frac{c_f b_f}{R_f} + \frac{1}{2}(A_{11f} t_f - 2B_{11f} c_f) \frac{m^2 \pi^2 b_f}{a^2} \right.$$

$$+ \left(A_{66f} t_f - 2B_{66f} c_f + B_{66f} \frac{t_f}{R_f} \right) \frac{n^2 \pi^2}{b_f}$$

$$\left. + \frac{1}{2} \left(A_{12f} t_f - 2B_{12f} c_f + B_{12f} \frac{t_f}{R_f} \right) \frac{n^2 \pi^2}{b_f} \right] \frac{m\pi}{4} \delta_{mr} \delta_{ns}$$

$$- 4 \left[\frac{1}{2} \left(A_{16f} t_f - 2B_{16f} c_f \right) \frac{r^2 \pi}{a} - A_{26f} \frac{c_f}{R_f} \frac{a}{\pi} \right.$$

$$+ \left(A_{16f} t_f - 2B_{16f} c_f + B_{16f} \frac{t_f}{R_f} \right) \frac{m^2 \pi}{a}$$

$$\left. + \frac{1}{2} \left(A_{26f} t_f - 2B_{26f} c_f + B_{26f} \frac{t_f}{R_f} \right) \frac{\pi s^2 a}{b_f^2} \right] \frac{nrs}{(m^2 - r^2)(n^2 - s^2)} \Delta_{mr} \Delta_{ns}$$

$$H_{6f}(m, n, r, s) = H_{5f}^{T}(m, n, r, s)$$

$$H_{7f}(m, n, r, s) = \left[-\left(A_{22f} + \frac{B_{22f}}{R_f}\right)\frac{c_f a}{R_f} + \frac{1}{2}\left(A_{12f}t_f - 2B_{12f}c_f + B_{12f}\frac{t_f}{R_f} - 2D_{12f}\frac{c_f}{R_f}\right)\frac{m^2\pi^2}{a}\right.$$

$$+ \left(A_{66f}t_f - 2B_{66f}c_f + 3B_{66f}\frac{t_f}{R_f} - 4D_{66f}\frac{c_f}{R_f} + 2D_{66f}\frac{t_f}{R_f^2}\right)\frac{m^2\pi^2}{a}$$

$$+ \frac{1}{2}\left(A_{22f}t_f - 2B_{22f}c_f + 2B_{22f}\frac{t_f}{R_f} - 2D_{22f}\frac{c_f}{R_f} + D_{22f}\frac{t_f}{R_f^2}\right)\frac{n^2\pi^2 a}{b_f^2}\right]\delta_{mr}\delta_{ns}$$

$$- 4\left[\left(A_{16f}\frac{t_f}{2} - B_{16f}c_f - 2D_{16f}\frac{c_f}{R_f} + B_{16f}\frac{t_f}{R_f}\right)\frac{\pi r^2 b_f}{a^2} - \left(A_{26f} + 2\frac{B_{26f}}{R_f}\right)\frac{c_f}{R_f}\frac{b_f}{\pi}\right.$$

$$+ \left(A_{26f}t_f - 2B_{26f}c_f + 2B_{26f}\frac{t_f}{R_f} - 2D_{26f}\frac{c_f}{R_f} + D_{26f}\frac{t_f}{R_f^2}\right)\frac{n^2\pi}{b_f}$$

$$+ \left.\left(A_{26f}\frac{t_f}{2} - B_{26f}c_f + 3B_{26f}\frac{t_f}{2R_f} - 2D_{26f}\frac{c_f}{R_f} + D_{26f}\frac{t_f}{R_f^2}\right)\frac{s^2\pi}{b_f}\right]\frac{mrs}{(m^2 - r^2)(n^2 - s^2)}\Delta_{mr}\Delta_{ns}$$

$$H_{8f}(m, n, r, s) = H_{7f}^{T}(m, n, r, s)$$

$$H_{9f}(m, n, r, s) = \left\{\frac{1}{R_f^2}A_{22f} + 2\left[\left(A_{22f} + \frac{B_{22f}}{R_f}\right)\frac{c_f t_f}{2R_f} - \frac{B_{22f}}{R_f}\right]\frac{n^2\pi^2}{b_f^2}\right.$$

$$- 2\left(A_{12f}\frac{c_f t_f}{2R_f} - \frac{B_{12f}}{R_f}\right)\frac{m^2\pi^2}{a^2}$$

$$+ \left(A_{11f}\frac{t_f^2}{4} - B_{11f}\frac{c_f t_f}{2} + D_{11f}\right)\frac{m^4\pi^4}{a^4}$$

$$+ \left[A_{22f}\frac{t_f^2}{4} - B_{22f}\frac{c_f t_f}{2} + D_{22f} + \left(2B_{22f} + \frac{D_{22f}}{R_f}\right)\frac{t_f^2}{2R_f} - D_{22f}\frac{c_f t_f}{2R_f}\right]\frac{n^4\pi^4}{b_f^4}$$

$$+ \left[A_{66f}t_f^2 - 2B_{66f}c_f t_f + 4D_{66f} + \left(2B_{66f} + \frac{D_{66f}}{R_f}\right)\frac{t_f^2}{R_f} - 4D_{66f}\frac{c_f t_f}{R_f}\right]\frac{m^2 n^2\pi^4}{a^2 b_f^2}$$

50

$$+ \left[A_{12f} \frac{t_f^2}{4} - B_{12f} c_f t_f + D_{12f} + B_{12f} \frac{t_f^2}{2R_f} - D_{12f} \frac{c_f t_f}{2R_f} \right] \frac{m^2 n^2 \pi^4}{a^2 b_f^2} \Bigg\} \frac{ab_f}{4} \; \delta_{mr} \delta_{ns}$$

$$- 4 \Bigg\{ \left[A_{16f} \frac{t_f^2}{2} - 2B_{16f} c_f t_f + 2D_{16f} \frac{t_f^2}{2R_f} - D_{16f} \frac{c_f t_f}{R_f} \right] \frac{(m^2 + r^2)\pi^2}{a^2}$$

$$- 2 \left[\left(A_{26f} + \frac{B_{26f}}{R_f} \right) \frac{c_f t_f}{R_f} - 2 \frac{B_{26f}}{R_f} \right]$$

$$+ \left[A_{26f} \frac{t_f^2}{2} + 2D_{26f} - 2 \left(B_{26f} + \frac{D_{26f}}{R_f} \right) c_f t_f + \left(2B_{26f} + \frac{D_{26f}}{R_f} \right) \frac{t_f^2}{2R_f} \right] \frac{(n^2 + s^2)\pi^2}{b_f^2} \Bigg\}$$

$$\frac{mnrs}{(m^2 - r^2)(n^2 - s^2)} \; \Delta_{mr} \Delta_{ns}. \tag{C5}$$

The coefficients a_{ij}^{kl} satisfy the symmetry relations

$$a_{ij}^{kl} = a_{ij}^{lk},$$

such that the assembled matrix $[A]$ is symmetric. The position indices i and j are related to the indices m, n, r and s by

$$i = N_\alpha (m - 1) + n$$

$$j = N_\alpha (r - 1) + s,$$

where

m, $r = 1, 2, \ldots, M_\alpha$ and n, $s = 1, 2, \ldots, N_\alpha$, $\alpha = 1$, 2, as defined in Equation 3.3.

For convenience in the numerical solution of the assembled matrix equations, the elastic stiffness matrix is partitioned into blocks corresponding to the vectors $\{X_1\}$ and $\{X_2\}$, as

$$
\begin{bmatrix}
A^{11} & A^{12} & A^{13} & A^{14} & A^{15} \\
 & A^{22} & A^{23} & A^{24} & A^{25} \\
 & & A^{33} & A^{34} & A^{35} \\
 & & & A^{44} & A^{45} \\
\text{symmetric} & & & & A^{55}
\end{bmatrix}
=
\begin{bmatrix}
A_{11} & A_{12} \\
A_{12}^{T} & A_{22}
\end{bmatrix}
\quad (C6)
$$

This form of the stiffness matrix corresponds to that used in Equation 3.5.

Definitions of the entries of the geometric stiffness matrix are made in a similar fashion. However, due to the assumption that the squares of the derivatives of the insurface displacements are small in comparison with the derivatives of the transverse slopes (see paragraph 2.3), the submatrices B_{11} and B_{12} are simply null matrices. The nonzero entries of B_{22} are calculated from

$$
b_{ij}^{22} = \sum_{f=1}^{2}\left[N_{xf}^{(o)} \frac{m^2\pi^2 b_f}{4a}\delta_{mr}\delta_{ns} - 8N_{xyf}^{(o)}\frac{mnrs}{(m^2 - r^2)(n^2 - s^2)}\Delta_{mr}\Delta_{ns}\right], \quad (C7)
$$

where i and j are related to m, n, r and s as noted previously. It should be noted that the expressions $N_{xf}^{(o)}$ and $N_{xyf}^{(o)}$ refer only to the relative magnitudes of the applied loads, since the intensity of each load is characterized by the single parameter λ (Equation 2.15).

The entries of B_{22} may be restated in terms of a single parameter for each load type by making the definitions

$$\overline{N}_x = \sum_{f=1}^{2} N_{xf}^{(o)} R_f / R_c$$

(C8)

$$\overline{N}_{xy} = \sum_{f=1}^{2} N_{xyf}^{(o)}.$$

Thus, the elements b_{ij}^{22} are

$$b_{ij}^{22} = \overline{N}_x \frac{m^2 \pi^2 b_c}{4a} \delta_{mr}\delta_{ns} - 8\overline{N}_{xy} \frac{mnrs}{(m^2 - r^2)(n^2 - s^2)} \Delta_{mr}\Delta_{ns}.$$